

# Contributions of lateral current path to p-n junction GaN-based LEDs performance

M. F. Othman, A. Abdul Aziz and M. R. Hashim

*Nano-Optoelectronics Research Technology and Laboratory, School of Physics, Universiti Sains Malaysia, 11800 Penang, Malaysia*

(Received 26 December 2007)

Homojunction GaN-based light emitting diodes (LEDs) with lateral geometry have been simulated by ISE TCAD. Due to lateral current injection, the knowledge in effective length of current path that leads to uniform current spreading across the active area is very important. In this regard, we studied the effect from various length of lateral current path on the device performance. We found that the current tended to crowd near to the edge of mesa sidewall due to high current density caused by undesirable length of current path. The current crowding generated localized thermal effects and degraded the device lifetime. Furthermore, the work revealed that the symmetry current spreading length exhibited better current distribution and higher output power.

## I. INTRODUCTION

In recent years, great progress has been made in the development of high-quality III-nitride electronics and optoelectronics devices. GaN-based light emitting diodes (LEDs) are one of the optoelectronics devices that attract the most attentions for blue-light emission, which is the base of white-light LEDs with yellow phosphors. LEDs are regarded as the most important light source in the next generation solid-state lightning owing to advantages in energy efficiency, long life, vivid colors, high reliability, environmental protection, safety and multiple applications [1-3]. However, the GaN-based LEDs have a critical weakness in its fabrication that involves the use of lateral carrier injection type due to the absence of appropriate conducting substrates. Due to the lateral device configuration, current crowding problem is often encountered and impedes the development of the efficient GaN-based LEDs.

Previously, Eliashevich *et al.* [4] reported that the conductivity of the n-type GaN layer should be of the same order as the transparent metal layer for uniform current spreading. Their model assumed the transparent metal layer to be a perfect current spreader where metal conducting layer have negligible resistance. However, further studies showed that certain parameters such as current density, the resistivities of the transparent electrode and n-type layers, and the effective length for lateral current path ( $l$ ) were also important factors in uniform current spreading [5,6]. The fact that a thin metal film has a much higher resistance than its corresponding bulk materials due to the reflection of conduction-electrons from defects that are trapped in the film during the deposition and from internal surfaces reveals the importance of transparent electrode in further current spreading model development [7].

Other investigations also revealed that the production of high efficient LEDs without the need of

transparent electrode are available by having good geometrical design [8]. Based on their models, they predicted that perfect uniform current spreading could be obtained with effective length of current path ( $l$ ) to p-electrode width ( $w$ ) ratio of LEDs approached zero.

However, their design was more complex, slightly hard to fabricate and ineffective cost for mass production. Thus, we tried to study the effect in a simpler method by just arranging the effective length of current path on the same LED dimension in order to optimize the current spreading inside the device.

In this paper, we use the ISE TCAD software to simulate the 3-D GaN LEDs with different lengths of current path between p-electrode and n-electrode. It is well known that 3-D simulation offer inexpensive, more reliable and more realistic way to study the effect of nano-scale differences in physical appearance which are difficult to determine by fabrication. With the structures and same contact characteristics, we varied the length of current path to investigate the effective length that optimizes the uniform current spreading in the devices. The simulation results show that the centre position of p-electrode on p-GaN layer exhibited better current distribution due to the symmetry in the current spreading length.

## II. METHODOLOGY

The schematics of the basic structure used for simulation are shown in Fig. 1. We have not defined a substrate for the structure but as mentioned previously, it could be a sapphire due to cost effectiveness and transparency to light extraction since other substrates such as SiC are more expensive and more absorptive than sapphire.

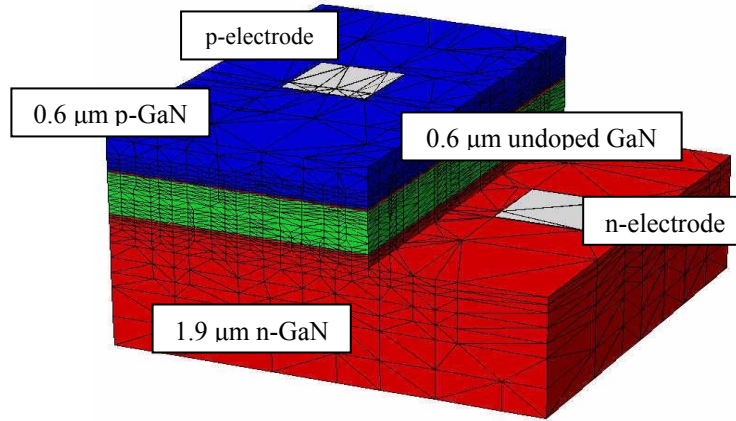


**FIG. 1.** The 3-D image of p-n junction GaN-based LED structure.

The structures were simulated using the ISE TCAD, simulation tool which is based on solving the Poisson and continuity equations for charge transport in semiconductor devices. The Poisson equation is given by

$$\nabla \varepsilon \cdot \nabla \varphi = -q(p - n + N_{D+} - N_{A-}), \quad (1)$$

where  $\varepsilon$  is electrical permittivity,  $\varphi$  is the electrostatic potential,  $q$  is the elementary electric charge,  $p$  is the hole density,  $n$  is the electron density,  $N_{D+}$  is the number of ionized donors, and  $N_{A-}$  is the number of ionized acceptors. The electron and hole continuity equations are given by

$$\nabla \cdot J_p = qR + q \frac{\partial p}{\partial t}, \quad (2)$$

$$\nabla \cdot J_n = qR + q \frac{\partial n}{\partial t}, \quad (3)$$

where  $R$  is net electron-hole recombination rate and  $J_{n,p}$  are the electron and hole current densities.

The position of n-electrode was maintained at the centre of n-GaN layer throughout the simulation while the position of p-electrode on p-GaN layer was varied from the mesa sidewall to the other end. Same parameters as used in previous work were applied [9]. The following physical models have been activated in our simulation; Philips unified mobility, Shockley-Read-Hall recombination, radiative recombination, bandgap narrowing at high doping levels, and thermodynamic model.

### III. RESULTS AND DISCUSSION

For our simulation, we had to scale down the real size of the device due to the limitation on computing capacity. However, the model outputs were already tested to be reliable and revealed the general view of current distribution and heat dissipation. We found that the emission wavelength for all structures are about 374 nm and shift toward shorter wavelength when forward current is increased due to the band filling effects of the deep localized energy states [10]. From the Fig. 2, the overall performance in term of current-voltage (I-V) and output power (L-V) was at the applied current point 1.5 μm compared to the rest when voltage applied at 5 V.

At this point, the p-electrode position was at the centre of the p-GaN layer. Due to the symmetry in the current spreading length, better current distribution inside the device was obtained [11]. We also noted that there was just slightly a difference in term of output power when the applied current point kept distance from the mesa sidewall. At this rate, we concluded that the lower possibility of leakage current to occur was at the longer length of lateral current path applied that helped the carriers to maximize the recombination process.

Fig. 3 shows characteristics of current density along x-axis for different selected lengths of current path. It indicates that, the 1.5 μm length of current path exhibited better current density behavior compared to the rest even though they shared the same profile. The difference about 0.5 μm between the lengths of current path didn't make any significant change except that the current density value became lower when the contact position situated far from the mesa edge. However, current density increased with increasing applied voltage. Thus, at high applied voltage, high current density could lead to current crowding localized area of the device especially at the mesa edge, resulting in the degradation of the device lifetime as a result of significant Joule heating.

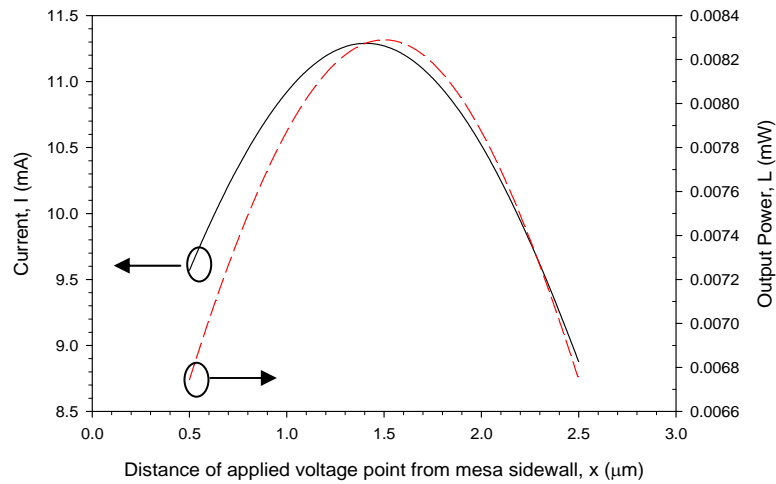


**FIG. 2.** The profile of I-V and L-V for LEDs with slanted mesa sidewall angles.

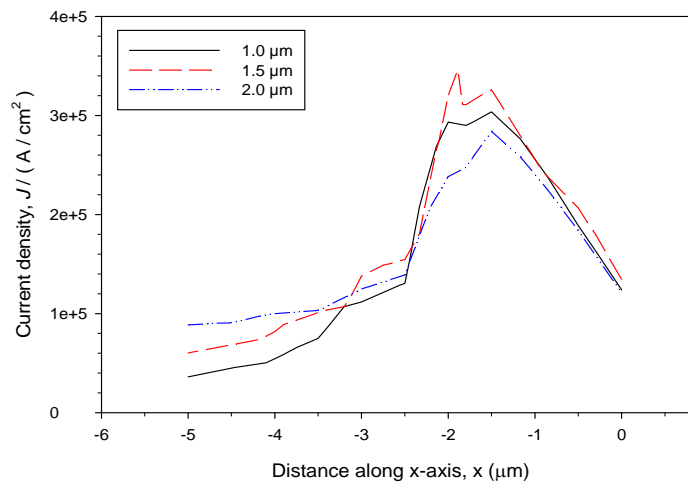


**FIG. 3.** The characteristic of current density along x-axis for different current path length.

Further investigation had been carried by setting certain operation temperature with the effective length of lateral current path, 1.5  $\mu\text{m}$  as shown in Fig. 4. At liquid nitrogen temperature (77 K), the device output power outperformed the output power of room temperature (300 K) by 548% while 824% difference when compared to the performance when it operated at 500 K. The emission wavelength of different operation temperatures at 77 K, 300 K and 500 K was 362  $\mu\text{m}$ , 374  $\mu\text{m}$  and 390  $\mu\text{m}$ , respectively. Higher bandgap energy was obtained when temperature increased. These phenomena lead to the variation of wavelength when different operating temperature applied. As the temperature increased, the Fermi level moved towards the middle of the gap so that Fermi level separation between the p- and n-side became smaller. As a result, higher I-V performance obtained at low temperature with the same voltage compared to others. Furthermore,

mobility of electron increased only due to scattering from ionized impurities occurred at low temperature while at higher temperature, the scattering affected by phonons [12]. Thus, the excessive thermal effects minimized by operating the device in low temperature.

#### IV. CONCLUSION

In summary, we demonstrated the contribution of lateral current path on p-n homojunction LEDs performance. We concluded that at 1.5  $\mu\text{m}$  where the p-electrode situated at the centre of p-type was the effective length of lateral current path where better current distribution obtained due to the symmetry of current spreading length. In addition, better performance also noted when LEDs operated at low temperature which resulted from their higher carriers' mobility.

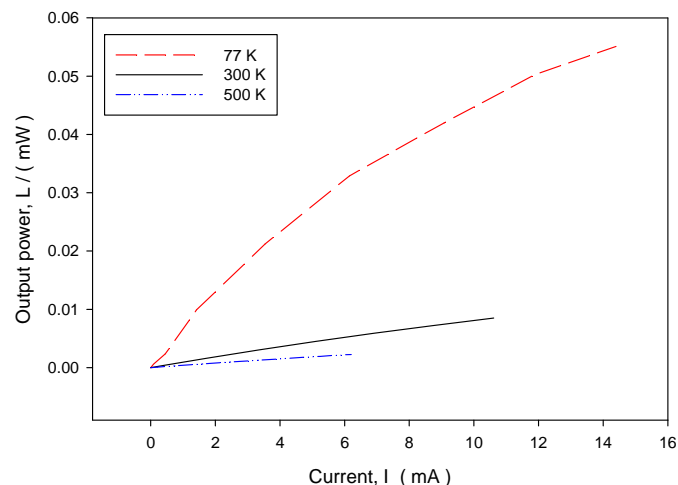


FIG. 4. I-V and L-V characteristics for different operating temperature at 5 V.

## ACKNOWLEDGMENTS

This work was conducted under Science Fund RMK-9 Research grant. The support from Institute of Graduate Studies, Universiti Sains Malaysia under Research University Fund for Graduates is fully gratefully acknowledged.

## REFERENCES

- [1] K. Gillessen and W. Schairer, *Light Emitting Diodes: An Introduction*, Prentice-Hall International, London (1987), pp. 209-236.
- [2] M. Yamada, T. Mitani, Y. Narukawa, S. Shioje, I. Niki, S. Sonobe, K. Deguchi, M. Sano and T. Mukai, *Jpn. J Appl. Phys.*, **41**, L1431 (2002).
- [3] H. G. Grimmeiss and J. W. Allen, *Journal of Non-Crystalline Solids*, **352**, 871-880 (2006).
- [4] I. Eliashevich, Y. Li, A. Osinsky, C. A. Tran, M. G. Brown and R. F. Karlicek Jr., *SPIE Conference on Light-Emitting Diodes: Research, Manufacturing and Applications-Part III*, **3621**, 28-36 (1999).
- [5] H. Kim, J. M. Lee, C. Huh, S. W. Kim, D. J. Kim, S. J. Park and H. Hwang, *Appl. Phys. Lett.*, **77**, 1903-1904 (2000).
- [6] H. Kim, S. J. Park and H. Hwang, *IEEE Trans. Electron Devices*, **48**, 1065-1069 (2001).
- [7] J. E. Siewenie and L. He, *J. Vac. Sci. Technol. A*, **17**, 1799-1804 (1999).
- [8] H. Kim, S. J. Park and H. Hwang, *IEEE Trans. Electron Devices*, **49**, 1715-1722 (2002).
- [9] M. F. Othman, A. Abdul Aziz and M. R. Hashim, *Proc. ICAMN*, 175 (2007).
- [10] T. Mukai, D. Morita and S. Nakamura, *Journal of Crystal Growth*, **189/190**, 778-781 (1998).
- [11] A. Ebong, S. Arthur, E. Downey, X. A. Cao, S. LeBoeuf and D. W. Merfeld, *Solid-State Electron*, **47**, 1817-1823 (2003).
- [12] T. T. Mnatsakanov, M. E. Levinshtein, L. I. Pomortseva, S. N. Yurkov, G. S. Simin and M. A. Khan, *Solid-State Electron*, **47**, 111-115 (2003).